# Evaluation of MU-MIMO Digital Beamforming Algorithms in B5G/6G LEO Satellite Systems

M. Rabih Dakkak*, Daniel Gaetano Riviello*, Alessandro Guidotti†, Alessandro Vanelli-Coralli*
*Dept. of Electrical, Electronic, and Information Engineering (DEI), Univ. of Bologna, Bologna, Italy
†National Inter-University Consortium for Telecommunications (CNIT), Univ. of Bologna Research Unit, Italy
{mrabih.dakkak2, daniel.riviello, a.guidotti, alessandro.vanelli}@unibo.it

***Abstract*—Satellite Communication (SatCom) systems will be a key component of 5G and 6G networks to achieve the goal of providing unlimited and ubiquitous communications and deploying smart and sustainable networks. To meet the ever-increasing demand for higher throughput in 5G and beyond, aggressive frequency reuse schemes (i.e., full frequency reuse), combined with digital beamforming techniques to cope with the massive co-channel interference, are recognized as a key solution. Aimed at (i) eliminating the joint optimization problem among the beamforming vectors of all users, (ii) splitting it into distinct ones, and (iii) finding a closed-form solution, we propose a beamforming algorithm based on maximizing the users' Signal-to-Leakage-and-Noise Ratio (SLNR) served by a Low Earth Orbit (LEO) satellite. We investigate and assess the performance of several beamforming algorithms, including both those based on Channel State Information (CSI) at the transmitter, i.e., Minimum Mean Square Error (MMSE) and Zero-Forcing (ZF), and those only requiring the users' locations, i.e., Switchable Multi-Beam. Through a detailed numerical analysis, we provide a thorough comparison of the performance in terms of per-user achievable spectral efficiency of the aforementioned beamforming schemes, and we show that the proposed SLNR beamforming technique is able to outperform both MMSE and ZF schemes in the presented SatCom scenario.**

***Index Terms*—Beyond 5G, 6G, Satellite Communications, MU-MIMO, Beamforming**

## I. Introduction and Motivation

Satellite Communication (SatCom) systems are expected to play a crucial role in future wireless networks. The integration of the Non-Terrestrial Network (NTN) component in the 5G ecosystem, envisaged in 3GPP Rel. 17, will improve the system flexibility, adaptability, and resilience, as well as extend the 5G coverage to rural, under- or un-served areas. SatCom is thus becoming an essential component to efficiently support the concept of wireless connectivity anywhere, anytime, and at any device. To completely enable this new role of SatCom systems, it is necessary to satisfy the user demand, in terms of different services, such as Internet of Things (IoT), and enhanced Mobile Broadband (eMBB), characterised by different performance requirements concerning rate and latency. In order to meet the demanding 5G requirements, both academia and industry have been focusing on advanced system-level techniques to increase the offered capacity. One approach is to better exploit the available spectrum, by either adding unused or underused spectrum chunks by means of flexible spectrum usage paradigms (e.g., Cognitive Radio solutions, [1]–[3]) or by fully exploiting the spectrum by decreasing the frequency reuse factor down to full frequency reuse (FFR) in multi-beam systems. Notably, the latter solution introduces substantial co-channel interference (CCI) from adjacent beams, thus necessitating the use of advanced interference management techniques, either at the transmitter-side, such as precoding and beamforming, [4]–[10], or at the receiver, such as Multi-User Detection (MUD) [11].

During the last years, the implementation of beamforming techniques in SatCom has been widely addressed for Geostationary Earth Orbit (GEO) systems, but also for Low Earth Orbit (LEO) constellations, as reported in [4]–[10] and the references therein. In these works, the main objective was to increase the overall throughput in unicast and/or multicast systems, also addressing well-known challenges for SatCom-based beamforming as scheduling and Channel State Information (CSI) retrieval. One of the most used techniques to increase the high demand of capacity is Multiuser Multiple-Input Multiple-Output (MU-MIMO). The design of hybrid beamforming algorithms for MU-MIMO communications in LEO systems has been recently addressed in [9]; here, the authors focused on a specific implementation of an on-board beamforming codebook compatible with 3GPP New Radio (NR). A thorough survey on MIMO techniques applied to SatCom is provided in [4], where both fixed and mobile satellite systems are examined and the major impairments related to the channel are identified. In the framework of MU-MIMO in SatCom, a critical challenge is the availability of CSI at the transmitter, especially in systems involving Non Geostationary Satellites (NGSO), as the one considered in this work. Such problem is also further compounded by the mobility of both the User Equipments (UEs) and the satellites, which can make the coherence time of the channel shorter than the transmission delay. The effect of non-ideal CSI at the transmitter, when applying beamforming in SatCom, is discussed in [12], where the authors proposed a novel MIMO scheme aimed at increasing the system sum-rate, availability, and variance performance.

In this paper, we design the transmit beamforming vectors based on the maximization of the Signal-to-Leakage-and-Noise Ratio (SLNR). This technique has been studied in Terrestrial Networks (TNs) and we investigate its application to a LEO satellite for Beyond 5G (B5G) and 6G communications. The proposed criterion aims at maximizing the received desired signal power for each user, while minimizing the

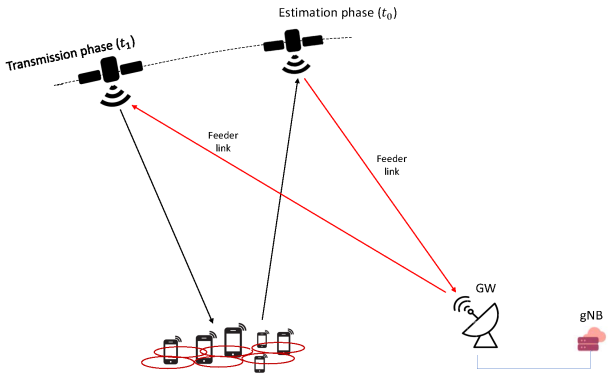


Fig. 1: System architecture with a single LEO satellite.

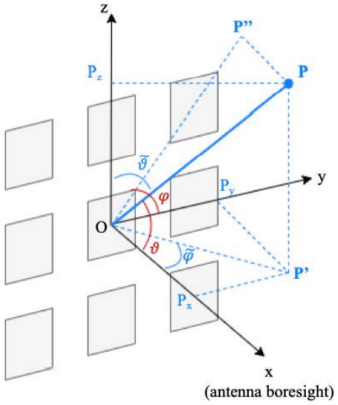


Fig. 2: coordinate system for the antenna array model.

overall interference power caused by each user to all other co-channel receivers. The resulting solution does not impose a restriction on the number of available transmit antennas and it determines the optimal procedure by solving a generalized eigenvalue problem [15]. The system level performance of the proposed algorithm is compared to benchmark beamforming schemes based on: i) the CSI knowledge at the transmitter, i.e., MMSE (Minimum Mean Square Error) and Zero Forcing (ZF); and ii) the users' location knowledge at the transmitter, i.e., Switchable Multi-Beam (MB) beamforming. Finally, unlike previous works, the satellite's movement is taken into account.

The remainder of the work is the following: Sec. II outlines the system model description and the assumptions, Sec. III introduces the proposed beamforming schemes. The numerical results and discussion are presented in Sec. IV, and finally, Sec. V concludes this work.

### A. Notation

Throughout this paper, and if not otherwise specified, the following notation is used: bold face lower case and bold face upper case characters denote vectors and matrices, respectively. $(\cdot)^T$ denotes the matrix transposition operator. $(\cdot)^H$ denotes the matrix conjugate transposition operator. $\mathbf{A}_{i,:}$ and $\mathbf{A}_{:,i}$ denote the $i$-th row and the $i$-th column of matrix $\mathbf{A}$, respectively. tr$(\mathbf{A})$ denotes the trace of matrix $\mathbf{A}$.

## II. System Model

We consider a single multi-beam LEO satellite at altitude $h_{sat}$ equipped with an on-board planar antenna array with $N$ radiating elements, providing connectivity to $K$ uniformly distributed on-ground UEs by means of $S$ beams. As previously mentioned, FFR is assumed and, thus, all beams use the same spectral resources. In the framework of NTN, in order to provide connectivity to the users, the LEO Satellite shall always maintain a logical link with an on-ground gNB; to this aim, the satellite is assumed to be either directly connected to an on-ground gateway (GW) or to be connected to other LEO satellites in the constellation by means of Inter-Satellite Links (ISLs). For the scope of this work, the two options are equivalent and are not further discussed in the following. It is worth mentioning that the adopted system architecture is thoroughly described in [16]. The LEO satellite is assumed to implement digital beamforming techniques. These techniques, detailed in the next section, require the estimation of either the CSI or the locations provided by the UEs. As shown in Fig. 1, these estimates are computed at a generic time instant $t_0$ in which the satellite is in a given orbital position. Then, the estimates are provided to the network entity for computing the beamforming coefficients, which in the following is assumed to be at the GW. Then, the beamforming coefficients are provided to the satellite to apply them to the symbols to be sent to the users. Thus, as represented in the architecture of Fig. 1, the actual beamformed transmission is performed at a time instant $t_1$. The latency $\Delta t = t_1 - t_0$ between the channel/location estimation phase and the transmission phase introduces a misalignment between the channel on which the beamforming matrix is computed and the actual channel through which the transmission occurs, which impacts the system performance. This latency can be computed as:

$$\Delta t = t_{ut,max} + 2t_{feeder} + t_p + t_{ad} \tag{1}$$

where: i) $t_{ut,max}$ is the maximum delay for the UEs requesting connectivity in the coverage area; ii) $t_{feeder}$ is the delay on the feeder link, considered twice since the estimates are to be sent to the GW on the return link and then the beamformed symbols are sent on the forward link to the satellite; iii) $t_p$ is the processing delay needed to compute the beamforming matrix; and iv) $t_{ad}$ includes any additional delay.

The antenna array model is based on ITU-R Recommendation M.2101, [6], and detailed in [7]. The coordinate system for the planar array is shown in Fig. 2. The planar array boresight direction is defined by the direction of the Sub Satellite Point (SSP). The center of the reference system is on-board the satellite at the center of the antenna array and P denotes the position of the on-ground UT, identified by the direction $(\tilde{\vartheta}, \tilde{\varphi})$, [6], [7]. In the following, we refer to the user direction in terms of the $(\vartheta, \varphi)$ angles, in which the boresight direction is $(0, 0)$ and that allows to easily derive the direction cosines for the considered user as follows: $u = \frac{P_y}{||P||} = \sin\vartheta\cos\varphi$,

$v = \frac{P_z}{||P||} = \sin\vartheta \sin\varphi$. Notably, the array radiation pattern in the generic $(\vartheta, \varphi)$ direction is given by the product of the antenna Array Factor (AF), $F(\vartheta, \varphi)$, and the single element radiation pattern, $g_E(\vartheta, \varphi)$, and it is computed as, [6], [7]:

$$g^{(tx)}(\vartheta, \varphi) = g_E(\vartheta, \varphi) F(\vartheta, \varphi) \tag{2}$$

where

$$F(\vartheta, \varphi) = \sum_{m=1}^{N_H} \sum_{q=1}^{N_V} e^{jk_0(md_H \sin\vartheta \cos\varphi + qd_V \sin\vartheta \sin\varphi)} \tag{3}$$

and

$$g^{(tx)}(u, v) = g_E(u, v) \sum_{m=1}^{N_H} \sum_{q=1}^{N_V} e^{jk_0(md_H u + qd_V v)} \tag{4}$$

In the above equations, $k_0 = 2\pi/\lambda$ is the wave number, $\lambda$ is the wavelength, $(N_H, N_V)$ denote the number of array elements on the horizontal ($y$-axis) and vertical $z$-axis directions, respectively, with $N = N_H N_V$ and $(d_H, d_V)$ denote the distance between adjacent array elements on the horizontal and vertical directions, respectively. Without affecting the generality of our analysis, we assume all of the radiating elements have the same radiation pattern $g_E(u, v)$.

The CSI vector, $\mathbf{h}_i = [h_{i,1}, ....h_{i,n}, ....., h_{i,N}]$, represents the channel between the $N$ radiating elements and the generic $i$-th on-ground UE, with $i = 1, ...K$. The generic channel coefficients between the $i$-th on-ground UE and the $n$-th on-board radiating element is given by:

$$h_{i,n} = g_{i,n}^{(tx)} g_{i,n}^{(rx)} = \frac{\lambda}{4\pi d_{i,n}} \sqrt{\frac{L_{i,n}}{\kappa B T_i}} e^{-j\frac{2\pi}{\lambda} d_{i,n}} \tag{5}$$

where: i) $d_{i,n}$ is the slant range between the $i$-th user and the $n$-th antenna feed, which for a single satellite can be assumed to depend only on the user index because the antenna array elements are co-located, i.e., $d_{i,n} = d_i$, $\forall n$; ii) $\kappa B T_i$ denotes the equivalent thermal noise power, with $\kappa$ being the Boltzmann constant, $B$ the user bandwidth which is assumed to be the same for all users, and $T_i$ the equivalent noise temperature of the $i$-th user receiving equipment; iii) $L_{i,n}$ denotes the additional losses considered between the $i$-th user and the $n$-th antenna feed (e.g., atmospheric and antenna cable losses) and, for a single satellite, we can assume $L_{i,n} = L_i$, $\forall n$; and iv) $g_{i,n}^{(tx)}, g_{i,n}^{(rx)}$ denote the transmitting and receiving complex antenna patterns between the $i$-th user and the $n$-th antenna feed. The additional losses are computed as:

$$L_i = L_{sha,i} + L_{atm,i} + L_{sci,i} + L_{CL,i} \tag{6}$$

where $L_{sha,i}$ represents the log-normal shadow fading term, $L_{atm,i}$ the atmospheric loss, $L_{sci,i}$ the scintillation, and $L_{CL,i}$ the Clutter Loss (CL), these terms are computed as per 3GPP TR 38.821 [17] and TR 38.811 [18]. Collecting all of the $K$ CSI vectors, the system-level $K \times N$ complex channel matrix $\mathbf{H}_{Sys}$ can be built, where the generic $i$-th row contains the CSI vector of the $i$-th user and the generic $n$-th column contains the channel coefficients from the $n$-th on-board feed towards the $K$ on-ground users. During each time frame, the Radio Resource Management (RRM) algorithm identifies a subset of $K_{sch}$ users to be served, leading to a $K_{sch} \times N$ complex scheduled channel matrix, $\mathbf{H} = \mathcal{F}(\mathbf{H}_{Sys})$, where $\mathcal{F}(\cdot)$ denotes the RRM scheduling function, which is a sub-matrix of $\mathbf{H}_{Sys}$, i.e., $\mathbf{H} \subseteq \mathbf{H}_{Sys}$, where contains only the rows of the scheduled users. The selected beamforming algorithm computes $N \times K_{sch}$ complex beamforming matrix $\mathbf{W}$ which projects $K_{sch}$ dimensional column vectors, $\mathbf{s} = [s_1, \ldots, s_{K_{sch}}]^T$ containing the unit-variance user symbols onto the $N$-dimensional space defined by the antenna feeds. The signal received by the $k$-th user can be expressed as follows:

$$y_k = \underbrace{\mathbf{h}_k \mathbf{W}_{:,k}\, s_k}_{\text{intended}} + \underbrace{\sum_{i=1, i\neq k}^{K_{sch}} \mathbf{h}_k \mathbf{W}_{:,i}\, s_i}_{\text{interfering}} + z_k \tag{7}$$

where $z_k$ is a circularly symmetric Gaussian random variable (r.v.) with zero mean and unit variance. The unit variance is motivated by observing that the channel coefficients in (5) are normalised to the noise power. The $K_{sch}$-dimensional vector of received symbols is:

$$\mathbf{y} = \mathbf{H}_{t_1} \mathbf{W}_{t_0} \mathbf{s} + \mathbf{z} \tag{8}$$

It shall be noticed that, as previously discussed, the channel matrix $\mathbf{H}_{t_0}$ is used to compute the beamforming matrix in the estimation phase at time instant $t_0$, while the beamformed symbols are sent to the users at a time instant $t_1$, in which the channel matrix is different and denoted as $\mathbf{H}_{t_1}$.

Based on the received symbols, the Key Performance Indicators (KPIs) of each scheduled user in each time frame can be obtained starting from the power transfer matrix as follows:

$$\mathbf{A} = |\mathbf{H}\mathbf{W}|^2 \tag{9}$$

This matrix contains the intended users' power on the diagonal elements, while the off-diagonal elements contain the interference received from each of the other users' signals. Based on $\mathbf{A}$, it is possible to compute the received Signal-to Noise Ratio (SNR) and Interference-to-Noise Ratio (INR) as follows:

$$SNR_k = a(k, k)$$
$$INR_k = \sum_{i=1, i\neq k}^{K_{sch}} a(k, i) \tag{10}$$

From (10) and (7), the Signal-to-Interference-plus-Noise Ratio (SINR) can be computed as:

$$SINR_k = \frac{SNR_k}{1 + INR_k} = \frac{||\mathbf{h}_k \mathbf{W}_{:,k}||^2}{1 + \sum_{i=1, i\neq k}^{K_{sch}} ||\mathbf{h}_k \mathbf{W}_{:,i}||^2} \tag{11}$$

From the above SINR, the spectral efficiency with which each user in each time frame is served can be obtained through the Shannon bound formula or based on the Modulation and Coding (ModCod) scheme for the considered air interface. In the following, we assume the former case, i.e.:

$$\eta_k = \log_2(1 + SINR_k) \tag{12}$$

## III. Digital beamforming schemes

In this section, we introduce linear beamforming algorithms focusing on those requiring knowledge of the CSI at the transmitter side, i.e., ZF and MMSE, and those requiring the UEs' locations, i.e., MB. Moreover, we also design the proposed SLNR-based beamforming algorithm. ZF and MMSE are known as linear beamforming techniques: ZF can be easily implemented by using the pseudo-inverse of the channel matrix and has optimal performance in high SNR regime; on the contrary, when users experience low SNRs, ZF suffers from noise enhancement and high performance degradation. MMSE overcomes the problem of ZF as it accounts for the noise by adding a regularisation factor in its expression. MMSE has indeed much better performance in low SNR regime.

### A. Benchmark beamforming algorithms

The following CSI/location based algorithms provide the performance benchmark for the assessment of the proposed SLNR-based beamforming.

*a) Zero Forcing (ZF):* The baseline implementation of the ZF algorithm is based on the inversion of the channel matrix $\mathbf{H}$, also known as Matched Filter (MF) beamforming. Notably, with this approach, the $\mathbf{H}^H\mathbf{H}$ matrix is often ill-conditioned, i.e., with a very large condition number, leading to a close-to-singular matrix. In these cases, the computation of the inverse matrix is prone to large numerical errors, resulting in a significant performance loss due to the inaccuracy of the matrix inversion; hence, to circumvent this issue, we focus on the following implementation of ZF [14]:

$$\mathbf{W}_{ZF} = (\mathbf{H}^H\mathbf{H})^{\dagger}\mathbf{H}^H \tag{13}$$

where $\dagger$ denotes the Moore-Penrose pseudo-inverse matrix. It is worth mentioning that ZF scheme suffers from noise enhancement, so that it can result in low SNR (SINR) since it does not take into account the noise power when implementing beamforming vectors. This impacts its performance as reported in the next section of numerical results.

*b) Minimum Mean Square Error (MMSE):* The MMSE precoder, or Regularized Zero Forcing (RZF), is designed to solve the MMSE problem as follows:

$$\mathbf{W}_{MMSE} = \arg\min_{\mathbf{W}} \mathrm{E}||\mathbf{HWs} + \mathbf{z} - \mathbf{s}||^2 \tag{14}$$

$$\mathbf{W}_{MMSE} = (\mathbf{H}^H\mathbf{H} + \mathrm{diag}(\boldsymbol{\alpha})\mathbf{I}_N)^{-1}\mathbf{H}^H \tag{15}$$

where $\mathbf{H}$ is the estimated channel matrix. In the above equation, $\boldsymbol{\alpha}$ is a vector of regularisation factors, with optimal value given by the inverse of the expected Signal-to-Noise Ratio (SNR) on the link [21]. Another aspect worth to be mentioned is that (15) leads to a large dimension of the Gram matrix $\mathbf{H}^H\mathbf{H}$, containing $N \times N$ coefficients. Hence, the authors in [1] proposed an alternative formulation that leads to a $K_{sch} \times K_{sch}$ matrix as follows:

$$\mathbf{W}_{MMSE} = \mathbf{H}(\mathbf{H}\mathbf{H}^H + \mathrm{diag}(\boldsymbol{\alpha})\mathbf{I}_{K_{sch}})^{-1} \tag{16}$$

The above formulation is computationally efficient since, notably, $K_{sch} < N$.

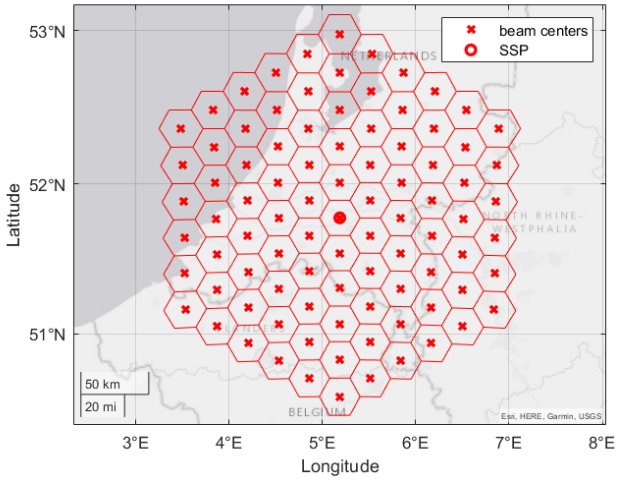


Fig. 3: Beam lattice in S-band with 5 tiers.

*c) Multi Beam (MB):* In this algorithm, [13], the beamforming vectors are computed in an approximated version, i.e., a pre-defined codebook of beamforming vectors built by: i) spatially sampling the coverage area, defining a given beam lattice on-ground identified by the beam center locations $c_q$; $q = 1, \cdots, S$ (as in the example provided in Fig. 3); and ii) computing the beamforming coefficients that are required to form signals with the required spatial signatures, i.e., to form beams in these directions. The pre-determined beamforming codebook is to be built as: $\mathbf{B} = [\mathbf{b}_1, \ldots, \mathbf{b}_q, \cdots, \mathbf{b}_S]$, where $\mathbf{b}_1$ contains all the $N$-dimensional beamforming vector which is steering the radiation pattern towards the 1-th beam center, and $\mathbf{b}_S$ is composed of the radiaion pattern of all $N$ antenna elements towards the center of the $\mathbf{b}_S$-th beam on ground and so on. For the generic $k$-th user to be served, its beamforming column vector in the beamforming matrix is identified as the column in the beamforming codebook corresponding to the closest beam center to the user's k location, i.e.,

$$\mathbf{W}_{MB} = [\mathbf{W}_{:,1}, \cdots, \mathbf{W}_{:,q}, \cdots, \mathbf{W}_{:,S}] \tag{17}$$

with

$$\mathbf{W}_{:,k} = \mathbf{B}_{:,j}$$
$$j = \arg\min_{i=1,\cdots,N} ||\mathbf{C}_i - \mathbf{P}_k||^2$$

where $\mathbf{C}_i$ the center of the $i$-th beam and $\mathbf{P}_k$ the position of the $k$-th user. It is worth mentioning that the MB approach is affected by the resolution of spatial sampling: the lower the number of beams, the larger the approximation and, thus, the worse the performance. Finally, it shall be noticed that when one user per beam is selected at each time frame, we obtain $K_{sch} = S$.

### B. Proposed SLNR-based beamforming

Given the power transfer matrix in (9), for a given user $k$, the co-channel interference (CCI) can be defined as the interference at the user $k$ that is caused by all other users, i.e.

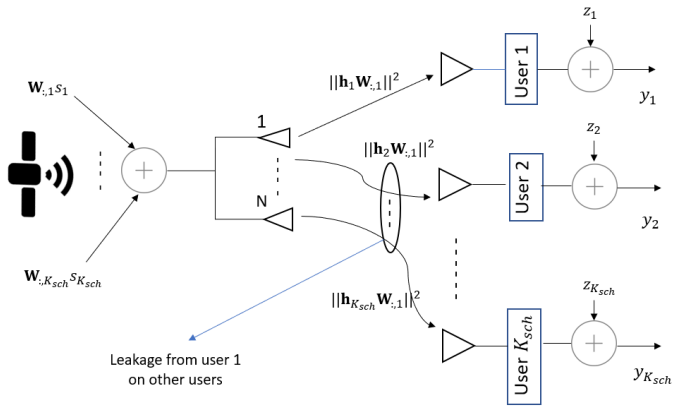


Fig. 4: Block diagram depicting the leakage from user 1 on other users.

$\sum_{i,i\neq k} a(k,i)$, while we refer to *leakage* to the interference that user $k$ causes to all other uses, i.e. $\sum_{i,i\neq k} a(i,k)$, it can be seen as a measure of how much signal power leaks into the other users. The problem of maximizing the SINR for all users in downlink beamforming has been extensively studied in [19] and no closed form solutions are available. The specific choice of one user's beamformer may affect the CCI experienced by other users, therefore the SINR values of all users are coupled and the beamformers must be jointly optimized.

In SLNR beamforming, the performance criterion for choosing the beamforming coefficients is based on maximizing the *signal-to-leakage-and-noise ratio* (SLNR) for all users simultaneously. This criterion leads to a decoupled optimization problem and admits an analytical closed form solution [15]. Unlike ZF scheme, SLNR-based beamforming considers the noise power in implementing beamforming vectors and does not require any dimension condition on the number of transmit/receive antennas. Furthermore, SLNR beamforming can be classified as a regularized channel inversion scheme, with regularization factors customized to each user based on their operating SNR, whereas the MMSE scheme employs the same regularization factor equal to the inverse of average SNR for all users [20].

In this paper, we consider single stream/layer based-design beamforming, i.e, each user terminal is equipped with single receiving antenna. Fig. 4 shows the block diagram of the leakage from user 1 on other users, considering a downlink multi-user environment with a single LEO satellite employing $N$ transmit antennas to serve $K_{sch}$ scheduled users. Considering (11), we note that the power of the desired signal component for user $k$ is given by $||\mathbf{h}_k\mathbf{W}_{:,k}||^2$. At the same time, the interfering power that is caused by the $k$-th user on the signal received by the generic $i$-th user is given by $||\mathbf{h}_i\mathbf{W}_{:,k}||^2$. Thus, we define such quantity, a leakage for user $k$, as the total power leaked from this user to all other users as follows:

$$\sum_{i=1,i\neq k}^{K_{sch}} ||\mathbf{h}_i\mathbf{W}_{:,k}||^2$$

For each user $k$, the intended signal power $||\mathbf{h}_k\mathbf{W}_{:,k}||^2$ is aimed to be large compared to the noise power at its receiver, and compared to the power leaked from such user to all other scheduled users, i.e., $\sum_{i=1,i\neq k}^{K_{sch}} ||\mathbf{h}_i\mathbf{W}_{:,k}||^2$. These considerations motivate to introduce a figure of merit in terms of SLNR as:

$$\text{SLNR}_k = \frac{||\mathbf{h}_k\mathbf{W}_{:,k}||^2}{1+\sum_{i=1,i\neq k}^{K_{sch}} ||\mathbf{h}_i\mathbf{W}_{:,k}||^2} \tag{18}$$

The SLNR expression can be rewritten for the sake of simplicity as:

$$\text{SLNR}_k = \frac{||\mathbf{h}_k\mathbf{W}_{:,k}||^2}{1+||\mathbf{Z}_k\mathbf{W}_{:,k}||^2} \tag{19}$$

where

$$\mathbf{Z}_k = [\mathbf{h}_1|\cdots|\mathbf{h}_{k-1}|\mathbf{h}_{k+1}|\cdots|\mathbf{h}_{K_{sch}}]$$

is an extended channel matrix that excludes $\mathbf{h}_k$ only. The beamforming matrix targeted for user $k$ that maximizes its SLNR is given by:

$$\hat{\mathbf{W}}_{:,k} = \arg\max_{\mathbf{W}} \text{SLNR}_k = \arg\max_{\mathbf{W}} \frac{||\mathbf{h}_k\mathbf{W}_{:,k}||^2}{1+||\mathbf{Z}_k\mathbf{W}_{:,k}||^2} \tag{20}$$

It is shown in [15] that the optimal beamformer is linked to closed-form solution of the generalized eigenvalue problem:

$$\hat{\mathbf{W}}_{:,k} \propto \text{max.eigenvector}((1+\mathbf{Z}_k^H\mathbf{Z}_k)^{-1}\mathbf{h}_k^H\mathbf{h}_k) \tag{21}$$

In terms of the eigenvector corresponding to the largest eigenvalue of the matrix $(1+\mathbf{Z}_k^H\mathbf{Z}_k)^{-1}\mathbf{h}_k^H\mathbf{h}_k)$, i.e., $\lambda_{max}$. The column vector $\hat{\mathbf{W}}_{:,k}$ shall be chosen according to (20), which results in the maximum SLNR value, i.e.,

$$\text{SLNR} = \lambda_{max}$$

Finally, as extensively detailed in [7], the power normalisation is a fundamental step for beamforming so as to properly take into account the power that can be emitted by both the satellite and per antenna. We consider the following three options for power normalisation:

1) the Sum Power Constraint (SPC): an upper bound is imposed on the total on-board power as:

$$\tilde{\mathbf{W}} = \frac{\sqrt{P_t}\mathbf{W}}{\sqrt{\text{tr}(\mathbf{W}\mathbf{W}^H)}} \tag{22}$$

$P_t$ being the total on-board power, which preserves the orthogonality of the beamformer columns but does not guarantee that the power transmitted from each feed will be upper bounded, i.e., it might be working in non-linear regime.

2) Per Antenna Constraint (PAC): the limitation is imposed per antenna with

$$\tilde{\mathbf{W}} = \sqrt{\frac{P_t}{N}}\ \text{diag}\left(\frac{1}{||\mathbf{W}_{1,:}||},\cdots,\frac{1}{||\mathbf{W}_{N,:}||}\right)\mathbf{W} \tag{23}$$

However, the orthogonality in the beamformer columns here is disrupted.

TABLE I: Simulation parameters.

| Parameter | Range |
|---|---|
| Carrier frequency | 2 GHz |
| System band | S (30 MHz) |
| Beamforming space | feed |
| Receiver type | VSAT |
| Receiver scenario | fixed |
| Propagation scenario | LOS, NLOS |
| System scenario | urban |
| Total on-board power density, $P_{t,\text{dens}}$ | (1,4,7) dBW/MHz |
| Number of tiers | 5 |
| Number of beams $S$ | 91 |
| Number of scheduled users $K_{Sch}$ | 91 |
| Number of transmitters $N$ | 1024 (32 $\times$32 UPA) |
| User density | 0.5 user/km$^2$ |

3) Maximum Power Constraint (MPC) solution:

$$\tilde{\mathbf{W}} = \frac{\sqrt{P_t}\mathbf{W}}{\sqrt{N \max_j ||\mathbf{W}_{j,:}||^2}} \tag{24}$$

the power per antenna is upper bounded and the orthogonality is preserved, but not the entire available on-board power is exploited. In this framework, it is worth highlighting that with the MB algorithm the three normalisation schemes lead to the same beamforming matrix, since the beamforming vectors are normalised by definition.

## IV. Numerical results

In this section, we report the outcomes of the numerical assessment based on the parameters reported in Table I, considering a single LEO satellite at $h_{sat} = 600$ km. The results are presented in terms of Cumulative Distribution Functions (CDFs) of the users' SINR and achievable spectral efficiency. The UEs, assumed to be at fixed locations, are uniformly distributed with a density of 0.5 users/Km$^2$, which corresponds to an average number of users $K = 28500$ to be served for each Monte Carlo iteration. The assessment is performed in full buffer conditions, i.e., infinite traffic demand. Based on these assumptions, the users are randomly scheduled. In particular, at each time frame one user for each beam is randomly selected and the total number of time frames is computed so as to guarantee all the users to be served. The numerical assessment is provided for SLNR-based beamforming and the performance is compared to the benchmark MMSE, ZF, and MB beamforming, assuming ideal CSI/location estimates at the transmitter side. Moreover, by considering Very Small Aperture Terminals (VSATs) as the receiver type, it is worth noticing that it has no advantage related to interference rejection with the directive radiation pattern, since it was supposed that all of the UEs' antennas are pointed towards the single satellite, with the assumption of co-located antenna feeds on the board. We first focus on Line Of Sight (LOS) propagation scenario in an urban environment, in which the channel coefficients include free space loss, log-normal shadow fading, atmospheric loss, and scintillation according to 3GPP TR 38.821, [17], and TR

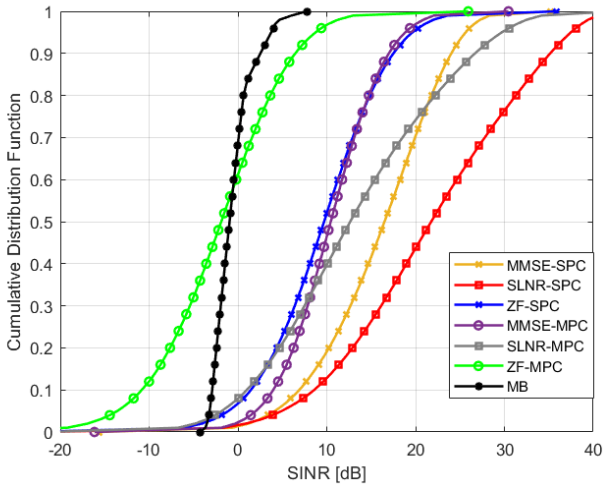


(a) SINR

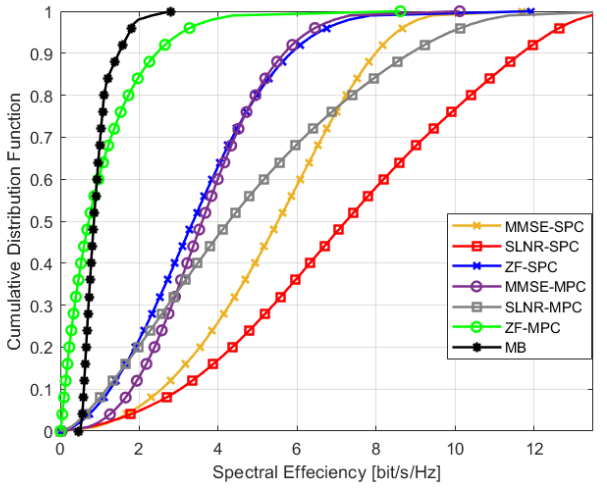


(b) Spectral efficiency

Fig. 5: SINRs and spectral efficiency CDFs for VSAT terminals in LOS scenario, at $P_t$ = 4 dBW/MHz.

38.811, [18]. Fig. 5 shows the CDFs of users' SINR and spectral efficiency for all the analyzed beamforming schemes with the SPC and MPC normalization. It is possible to observe that the proposed SLNR-based beamforming provides a better performance than MMSE, followed by ZF and MB, where ZF with SPC shows a better performance with respect to MB. In terms of normalization, SPC is considered the best. However, SPC does not guarantee that each antenna element or feed does not exceed the power it may emit and, thus, the MPC and PAC solutions could be preferred. When comparing them, it can be noticed that the MPC performs significantly better especially when the interference in the system is larger, i.e., for large values of transmission power and with VSAT terminals that have large antenna gains: in such cases, it is fundamental to maintain the orthogonality in the beamforming

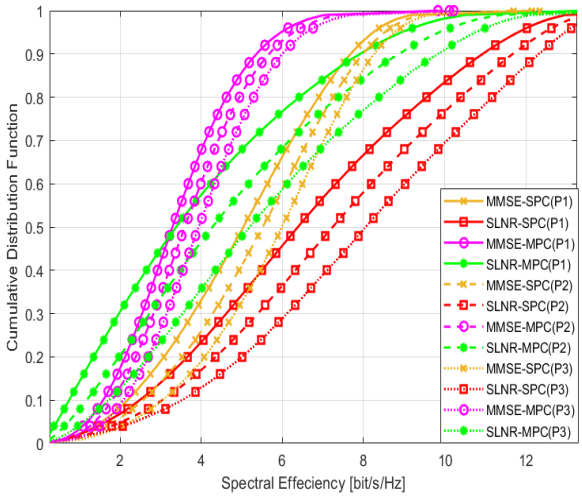


Fig. 6: Spectral efficiency CDFs in LOS scenario for SLNR and MMSE beamforming at different power density values, $P_1 = 1$ dBW/MHz (solid line), $P_2 = 4$ dBW/MHz (dashed line), and $P_3 = 7$ dBW/MHz (dotted line).

matrix columns. Hence, for all beamforming algorithms, PAC provides the worst performance scenario and, thus, we will focus in the analysis only on SPC and MPC normalization.

Fig. 6 reports a comparison in the spectral efficiency performance of the SLNR and MMSE beamforming when considering different values of the transmitted power density $P_t = \{1, 4, 7\}$ dBW/MHz. It can be noticed that by doubling the transmitted power for SLNR scheme, we get a gain in the order of 0.85-0.95 bit/sec/Hz, and for MMSE in order 0.4-0.5 bit/sec/Hz. Such results give additional advantage of superiority of SLNR performance algorithm. However, the case is different for PAC, a larger transmission power leads to a worse spectral efficiency denoting a significant sensitivity to the loss of orthogonality in the beamforming matrix columns in the increased interference scenario.

To conclude the assessment of this work, we investigate NLOS (Non Line of Sight) propagation conditions in an urban environment. In addition to the channel impairments already present in the LOS scenario, the user experiences Clutter Loss (CL), [17], [18]. The distribution of users' SINRs and spectral efficiencies for all the considered beamforming schemes in NLOS scenario are reported in Fig. 7. It is possible to observe that the proposed SLNR-based beamforming scheme provides again better performance than MMSE, followed by MB. In this case ZF has the worst behavior motivated by its high sensitivity to the shadowing and clutter loss. The superiority of SLNR beamforming over MMSE in both (LOS and NLOS) scenario is motivated by the fact that SLNR uses a customized regularization factor for each user, whereas the MMSE scheme employs the same regularization factor for all of them [20]. This becomes a crucial factor in the presented SatCom scenario, where users experience non-uniform and highly-variable SNRs. Fig. 8 shows that the performance significantly gets

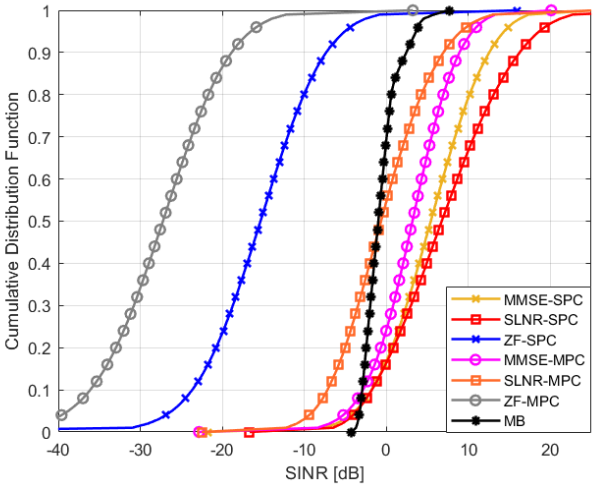


(a) SINR

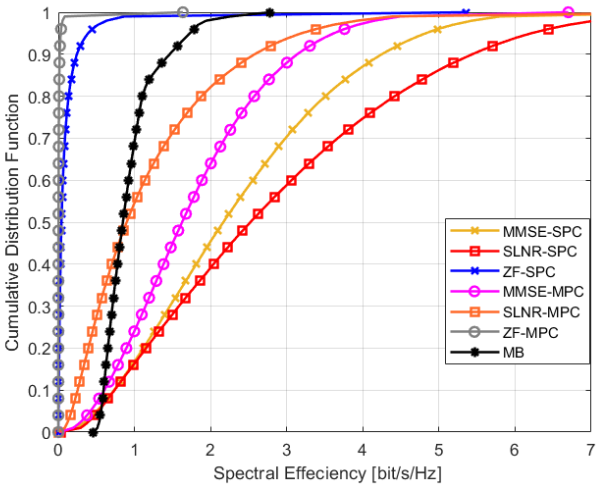


(b) Spectral efficiency

Fig. 7: SINRs and spectral efficiency CDFs for VSAT terminals in NLOS scenario, at $P_t$ = 4 dBW/MHz.

worse in NLOS conditions compared to the beamforming in LOS scenario, with spectral efficiency degradation in the order of 4-5 bit/s/Hz for SLNR-based beamforming and in the order of 3-4 bit/s/Hz for MMSE-SPC and, finally, 1-2 bit/s/Hz for MMSE-MPC.

## V. Conclusions

In this work, we proposed and assessed a beamforming algorithm in LEO SatCom system based on maximizing the figure of merit (SLNR) which eliminates the joint coupling between the beamforming vectors into multiple separate optimization problems of the targeting users. We compared its performance to CSI and non-CSI based benchmark algorithms (MMSE and ZF) and MB, respectively. The numerical results provided a significant better performance of SLNR-based beamforming than the optimal MMSE followed by

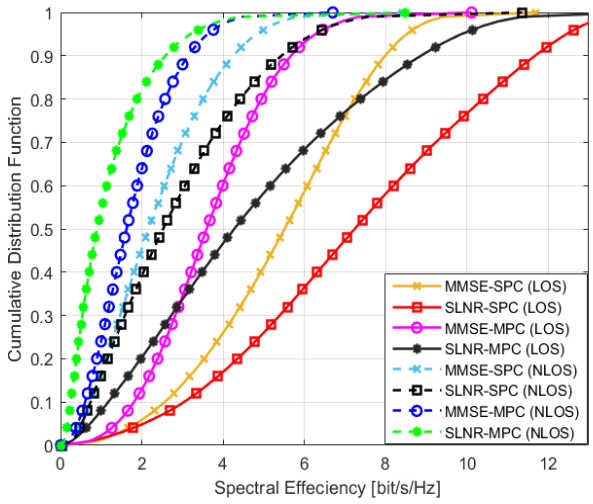


Fig. 8: Spectral efficiency CDFs considering only MMSE and SLNR beamforming scenario at $P_t$ = 4 dBW/MHz in LOS scenario (solid line) and NLOS scenario (dashed line).

MB and ZF beamforming in terms of spectral efficiency and SINR. As for the normalisations, SPC introduced the best performance for all beamforming algorithms followed by MPC, and PAC was the worst. The analysis showed a degradation in the performance when moving from LOS to NLOS propagation scenario. Finally, the increased transmitted power density introduced slight improvement for SLNR and MMSE beamforming. Future works shall take into account multiple satellites in a mega-constellation scenario targeting global coverage.

## VI. Acknowledgments

This work has been funded by the European Union Horizon-2020 Project DYNASAT (Dynamic Spectrum Sharing and Bandwidth-Efficient Techniques for High-Throughput MIMO Satellite Systems) under Grant Agreement 101004145. The views expressed are those of the authors and do not necessarily represent the project. The Commission is not liable for any use that may be made of any of the information contained therein.

## References

[1] V. Icolari, A. Guidotti, D. Tarchi, and A. Vanelli-Coralli, "An interference estimation technique for satellite cognitive radio systems", in *2015 IEEE International Conference on Communications (ICC)*, 2015,pp. 892–897.

[2] S. Chatzinotas, B. Evans, A. Guidotti, V. Icolari, E. Lagunas, S. Maleki, S. K. Sharma, D. Tarchi, P. Thompson, and A. Vanelli-Coralli, "Cognitive approaches to enhance spectrum availability for satellite systems", *International Journal of Satellite Communications and Networking*, vol. 35, no. 5, pp. 407–442, 2017.

[3] K. Liolis, G. Schlueter, J. Krause, F. Zimmer, L. Combelles, J. Grotz, S. Chatzinotas, B. Evans, A. Guidotti, D. Tarchi et al., "Cognitive radio scenarios for satellite communications: The corasat approach", in *2013 Future Network & and Mobile Summit. IEEE*, 2013, pp. 1–10.

[4] P.-D. Arapoglou, K. Liolis, M. Bertinelli, A. Panagopoulos, P. Cottis, and R. De Gaudenzi, "Mimo over satellite: A review", *IEEE communications surveys & tutorials*, vol. 13, no. 1, pp. 27–51, 2010.

[5] L. You, K.-X. Li, J. Wang, X. Gao, X.-G. Xia, and B. Ottersten, "Massive MIMO transmission for LEO satellite communications", *IEEE Journal on Selected Areas in Communications*, vol. 38, no. 8, pp. 1851–1865, 2020.

[6] A. Guidotti and A. Vanelli-Coralli, "Clustering strategies for multicast Beamforming in multibeam satellite systems", *International Journal of Satellite Communications and Networking*, vol. 38, no. 2, pp. 85–104, 2020.

[7] ——, "Design trade-off analysis of Beamforming multi-beam satellite communication systems", in *2021 IEEE Aerospace Conference (50100)*, 2021, pp. 1–12.

[8] ——, "Geographical scheduling for multicast Beamforming in multibeam satellite systems", in *2018 9th Advanced Satellite Multimedia Systems Conference and the 15th Signal Processing for Space Communications Workshop (ASMS/SPSC)*, 2018, pp. 1–8.

[9] J. Palacios, N. Gonzalez-Prelcic, C. Mosquera, T. Shimizu, and ´C.-H. Wang, "A hybrid beamforming design for massive MIMO LEO satellite communications", *Frontiers in Space Technologies*, vol. 2, 2021. [Online]. Available: https://www.frontiersin.org/article/10.3389/frspt.2021.696464

[10] G. Caire, M. Debbah, L. Cottatellucci, R. De Gaudenzi, R. Rinaldo, R. Mueller, and G. Gallinaro, "Perspectives of adopting interference mitigation techniques in the context of broadband multimedia satellite systems", in *ICSSC 2005, 23rd AIAA International Communications Satellite Systems Conference*, 2005.

[11] G. Colavolpe, A. Modenini, A. Piemontese, and A. Ugolini, "Multiuser detection in multibeam satellite systems: Theoretical analysis and practical schemes", *IEEE Transactions on Communications*, vol. 65, no. 2, pp. 945–955, 2016.

[12] N. Zorba, M. Realp, and A. I. Perez-Neira, "An improved partial CSIT ´random beamforming for multibeam satellite systems", in *2008 10th International Workshop on Signal Processing for Space Communications*, 2008, pp. 1–8.

[13] P. Angeletti and R. De Gaudenzi, "A pragmatic approach to massive MIMO for broadband communication satellites", *IEEE Access*, vol. 8, pp. 132212–132236, 2020.

[14] A. Guidotti, C. Sacchi and A. Vanelli-Coralli, "Feeder Link Beamforming for Future Broadcasting Services: Architecture and Performance", in *IEEE Transactions on Aerospace and Electronic Systems*, doi: 10.1109/TAES.2022.3144243.

[15] M. Sadek, A. Tarighat and A. H. Sayed, "A Leakage-Based Beamforming Scheme for Downlink Multi-User MIMO Channels", in *IEEE Transactions on Wireless Communications*, vol. 6, no. 5, pp. 1711-1721, May 2007, doi: 10.1109/TWC.2007.360373.

[16] A. Guidotti, C. Amatetti, F. Arnal, B. Chamaillard and A. Vanelli-Coralli. "Location-assisted Beamforming in 5G LEO systems: architectures and performances", EuCNC 2022.

[17] 3GPP, "38.821 -Solutions for NR to support Non-Terrestrial Networks (NTN)", Jun. 2021.

[18] ——, "38.811 - Study on New Radio (NR) to support non-terrestrial networks", 2020.

[19] M. Schubert and H. Boche, "Solution of the multiuser downlink beamforming problem with individual SINR constraints", *IEEE Trans. Veh. Technol.*, vol. 53, no. 1, pp. 18–28, Jan. 2004.

[20] P.Patcharamaneepakorn, S. Armour and A. Doufexi, "On the Equivalence Between SLNR and MMSE Precoding Schemes with Single-Antenna Receivers," in IEEE Communications Letters, vol. 16, no. 7, pp. 1034-1037, July 2012, doi: 10.1109/LCOMM.2012.050912.120329.

[21] R. Muharar, J. Evans, "Downlink Beamforming with Transmit-side Channel Correlation: A Large System Analysis," IEEE Int. Conf. on Commun. (ICC), Jun. 2011.